Biophysical Journal, Volume *122*

Supplemental information

Molecular basis of PIP2-dependent conformational switching of phosphorylated CD44 in binding FERM

Meina Ren, Lina Zhao, Ziyi Ma, Hailong An, Siewert Jan Marrink, and Fude Sun

Supplemental information

Molecular Basis of PIP2-dependent Conformational Switching of Phosphorylated CD44 in binding FERM

Meina Ren[1], Lina Zhao[1], Ziyi Ma[1], Hailong An[1]*, Siewert Jan Marrink[2]*, Fude Sun[1]*

1 Key Laboratory of Molecular Biophysics, Hebei Province, Institute of Biophysics, School of Health Science & Biomedical Engineering, Hebei University of Technology, Tianjin, China

2 Groningen Biomolecular Sciences and Biotechnology Institute, University of Groningen, Nijenborgh 7, 9747AG Groningen, The Netherlands

*Correspondence: sunfd@hebut.edu.cn (F.S.); s.j.marrink@rug.nl (S.J.M.); hailong_an@hebut.edu.cn (H.A.).

Table S1. GROMACS itp files of phosphoserine

```
[ moleculetype ]
; Name                 Exclusions
   Phosphoserine       1
[ atoms ]
   1       P2       1   SP2   BB   1    0.0000
   2       P1       1   SP2   SC1  2    0.0000
   3       Qa       1   SP2   PO4  3   -2.0000
[ bonds ]
; Sidechain bonds
   1       2        1  0.255   7500
   2       3        1  0.225   5000
[ angles ]
; Sidechain angles
   1   2   3        2   90.0   50.0
```

Movie S1. The process of S325 phosphorylated CD44 debinding to FERM during umbrella sampling.

Supporting Figures:

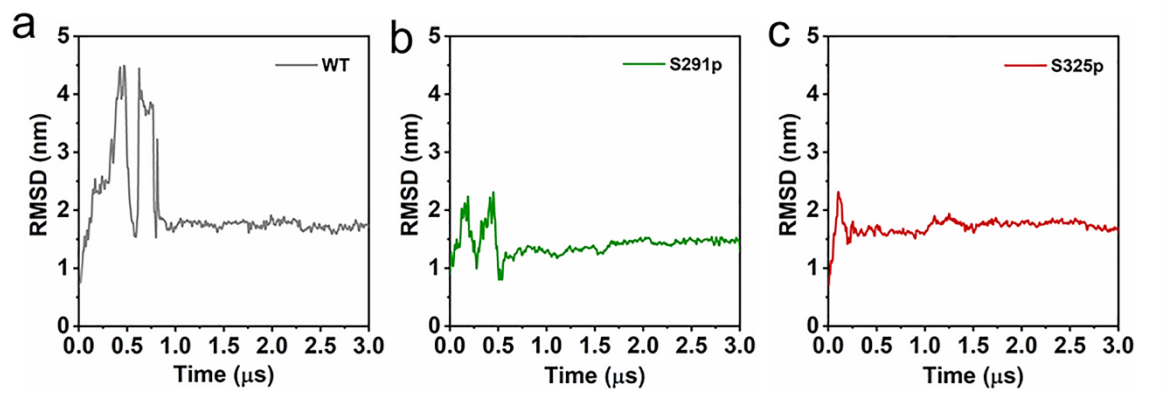

FIGURE S1. RMSD of different phosphorylated CD44 binding to FERM in a 95% POPC/5% PIP2 lipid environment.

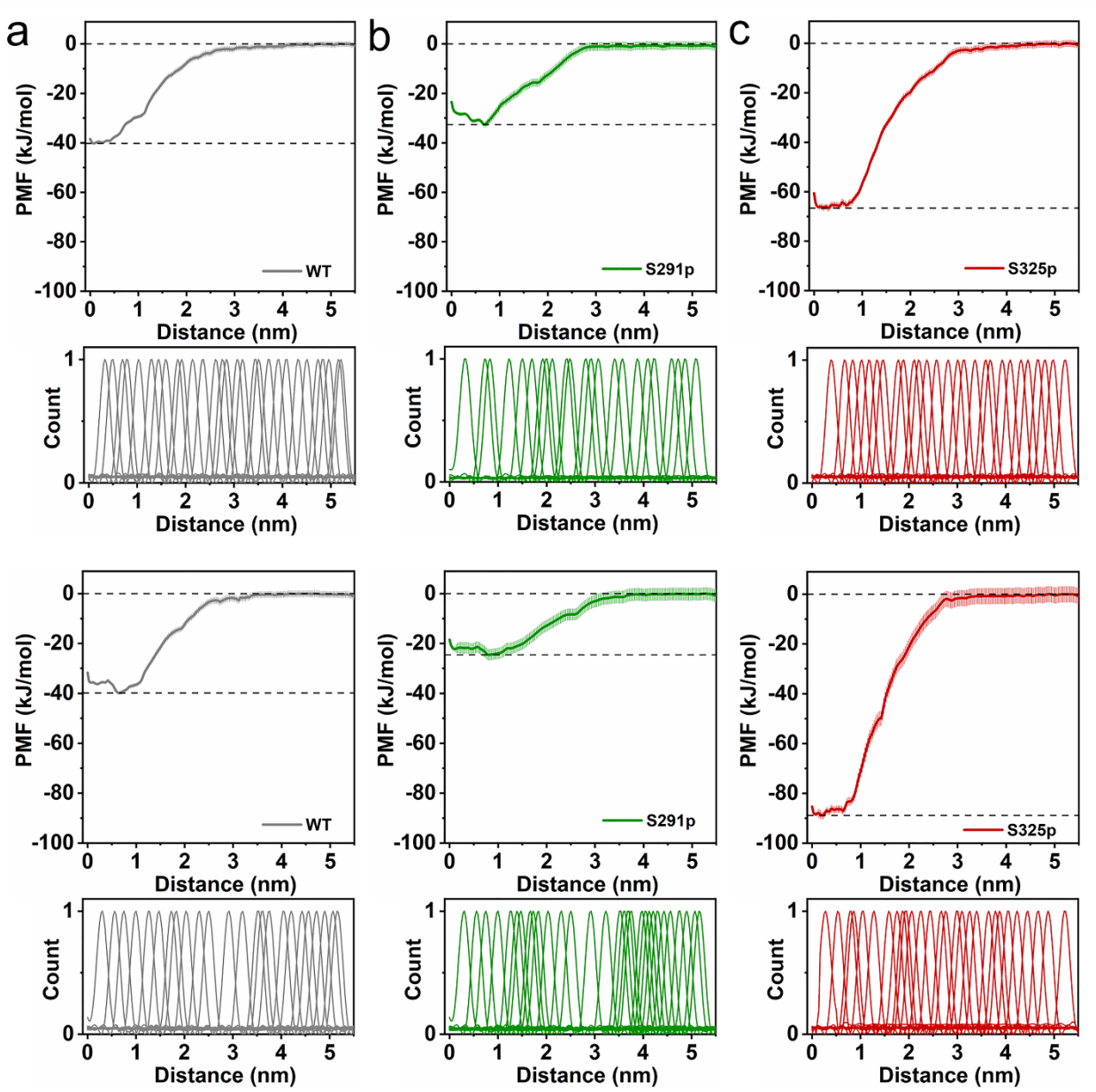

FIGURE S2. Potentials of mean force for CD44-CTD/FERM interactions under (a) WT, (b) S291p and (c) S325p. The upper and lower panels represent PMF results of two randomly selected proteins stably binding conformations. The two broken horizontal lines define the depth of the energy well corresponding to the minimum of the PMF. The corresponding histograms from the individual umbrella sampling window are shown beneath the PMF in order to demonstrate overlap.

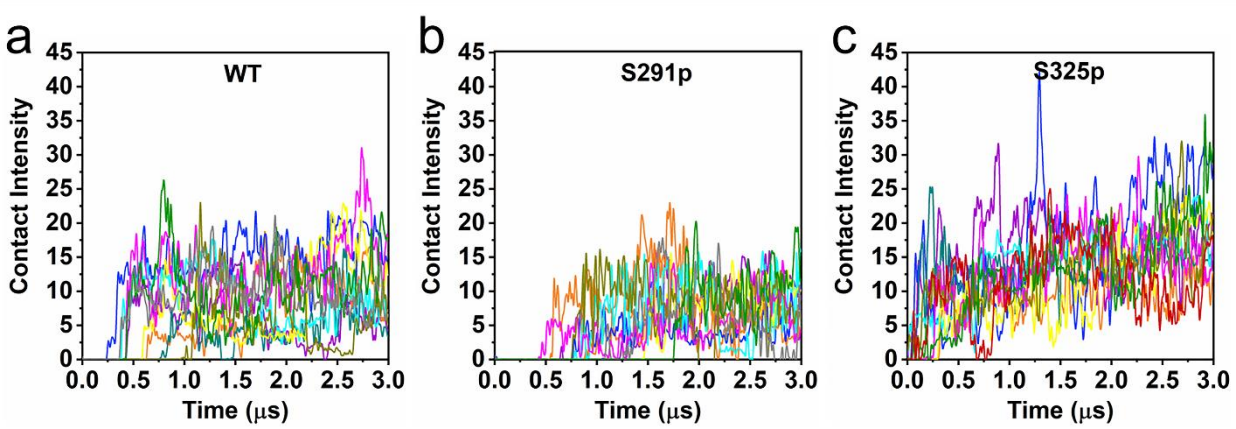

FIGURE S3. Contact intensity of CD44 with FERM for each sample of the (a) WT, (b) S291p and (c) S325p CD44 phosphorylation states in 95% POPC/5% PIP2 membrane environment.

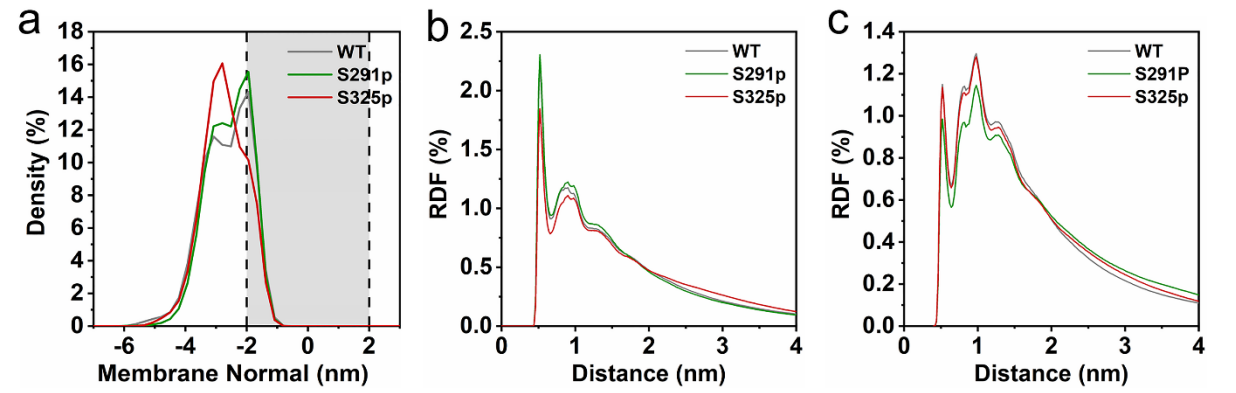

FIGURE S4. Phospholipid interactions of CD44 in systems 95% POPC/5% PIP2 with FERM. (a) The density distributions of CTD along the membrane normal at the three phosphorylation conditions. (b) A comparison of radial distribution functions (RDF) of PIP2 lipids relative to CD44-CTD under different phosphorylation modifications. (c) A comparison of RDF of PIP2 lipids relative to CD44-TMD under different phosphorylation modifications.

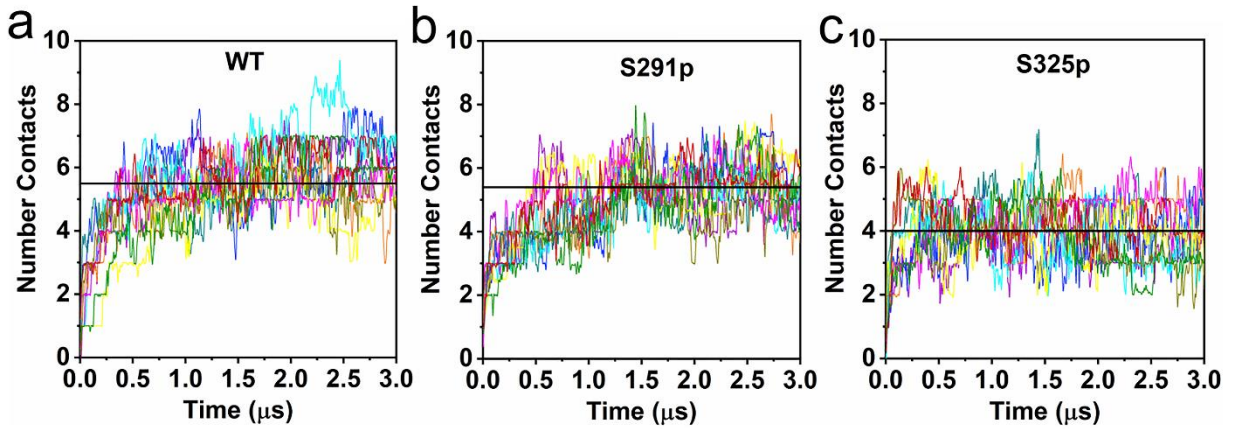

FIGURE S5. Number of contacts between CTD and PIP2 for each sample of the (a) WT, (c) S291p and (c) S325p CD44 phosphorylation states in systems 95% POPC/5% PIP2 with FERM. The solid black lines represent the mean of the 10 replicas.

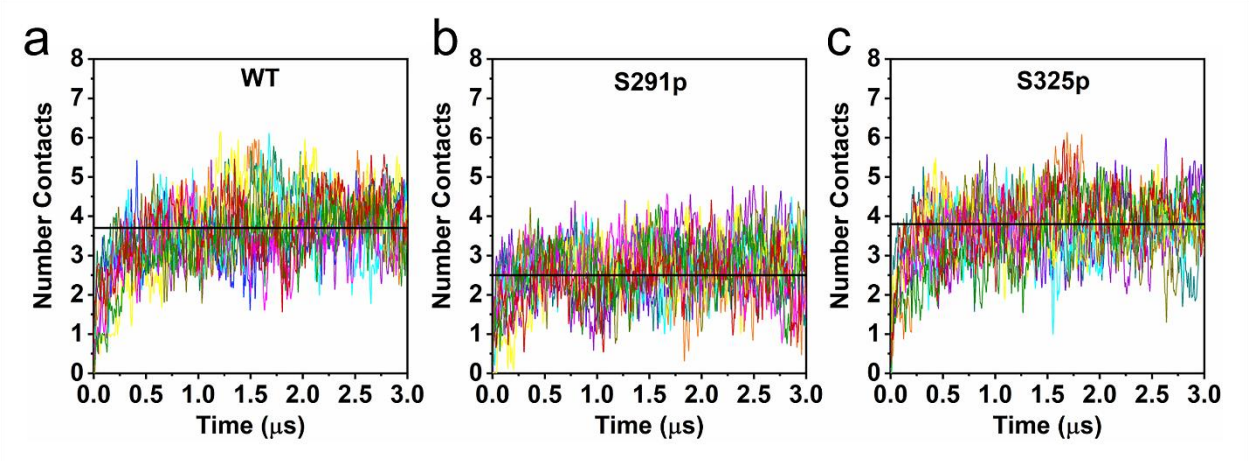

FIGURE S6. Number of contacts between TMD and the lipids of PIP2 for each sample of the (a) WT, (b) S291p and (c) S325p CD44 phosphorylation states in systems 95% POPC/5% PIP2 with FERM. The solid black lines represent the mean of the 10 replicas.

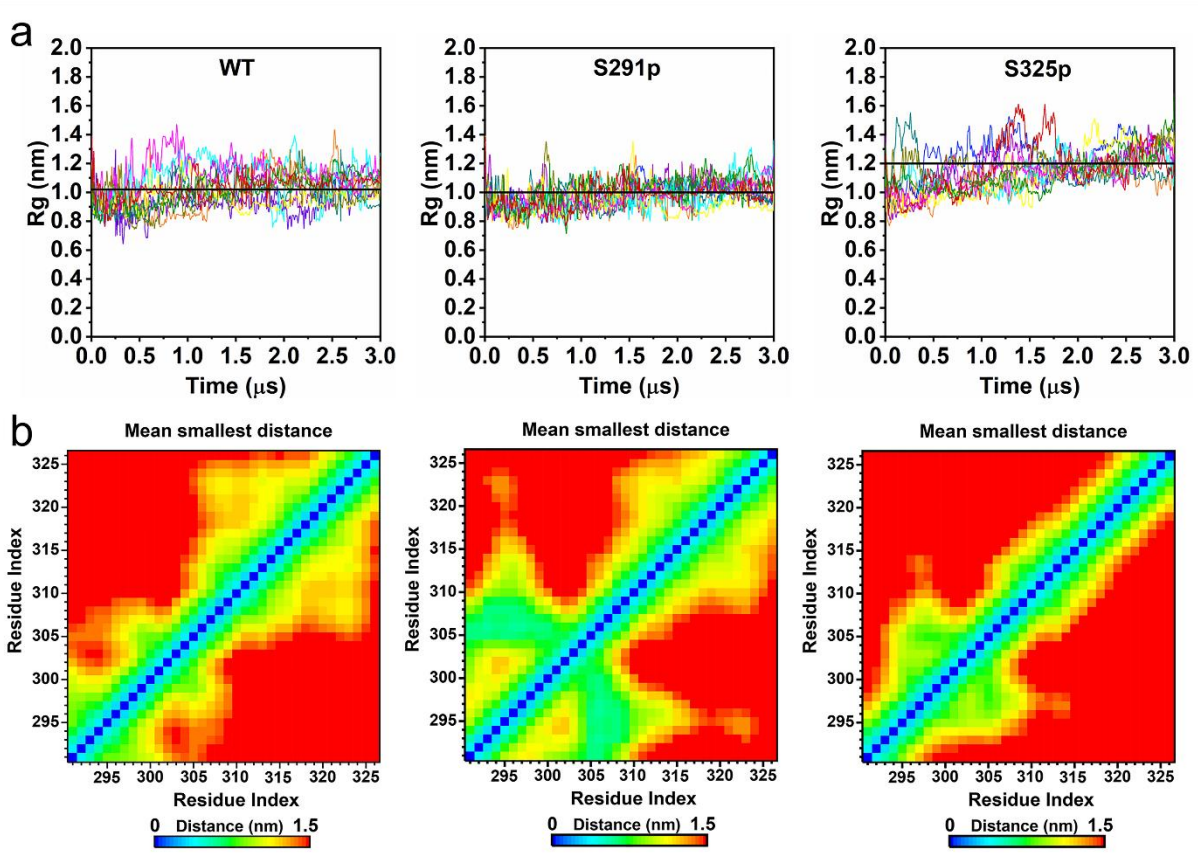

FIGURE S7. Structural folding differences of CD44 in systems 95% POPC/5% PIP2 with FERM. (a) Radius of gyration of the CTD for each sample of the WT (left), S291p (middle) and S325p CD44-S325p (right) CD44 phosphorylation conditions. The solid black lines represent the mean of the 10 replicas. (b) Interactions between all residues of CTD evaluated as average minimum distances between CTD residues over the simulation time and all simulations of a given type. All maps are rainbow colored blue to red, for distances from 0 to 1.5 nm and larger. Data obtained from 10 independently replicated MD simulations, first 500 ns were excluded from the analysis for equilibration purposes.

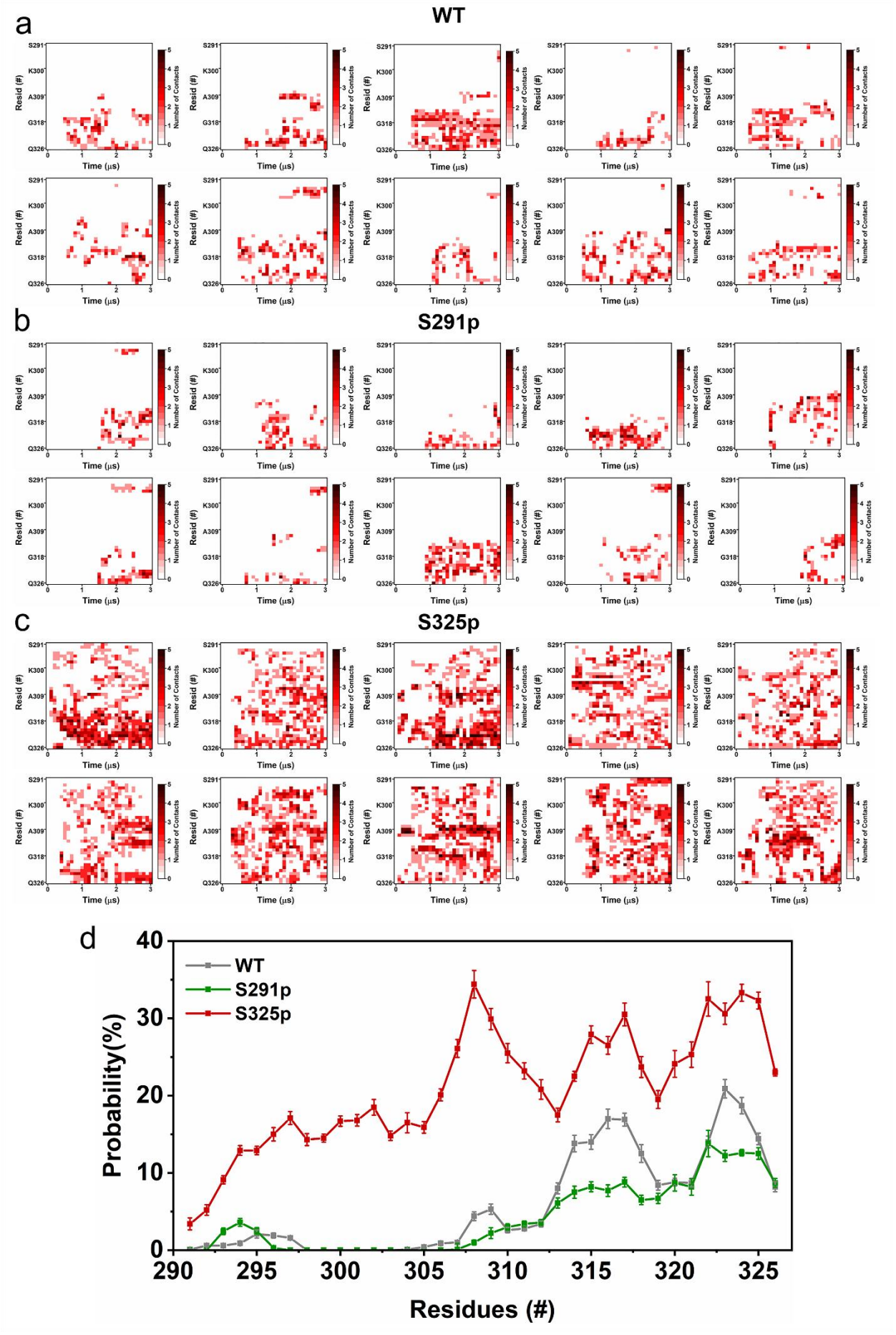
a
WT
b
S291p
c
S325p
Resid (#)
S291
K300
A309
G318
Q326
Time (μs)
Number of Contacts
d
WT
S291p
S325p
Probability(%)
Residues (#)
0
10
20
30
40
290
295
300
305
310
315
320
325

FIGURE S8. Contact heatmap plots between amino acids of CD44-CTD and FERM during the entire 3 μs simulation for each sample of the (a) WT, (b) S291p and (c) S325p CD44 phosphorylation states in 95% POPC/5% PIP2 membrane environment. (d) The probability distribution of the CTD residues in different phosphorylation states to be in contact with the FERM.

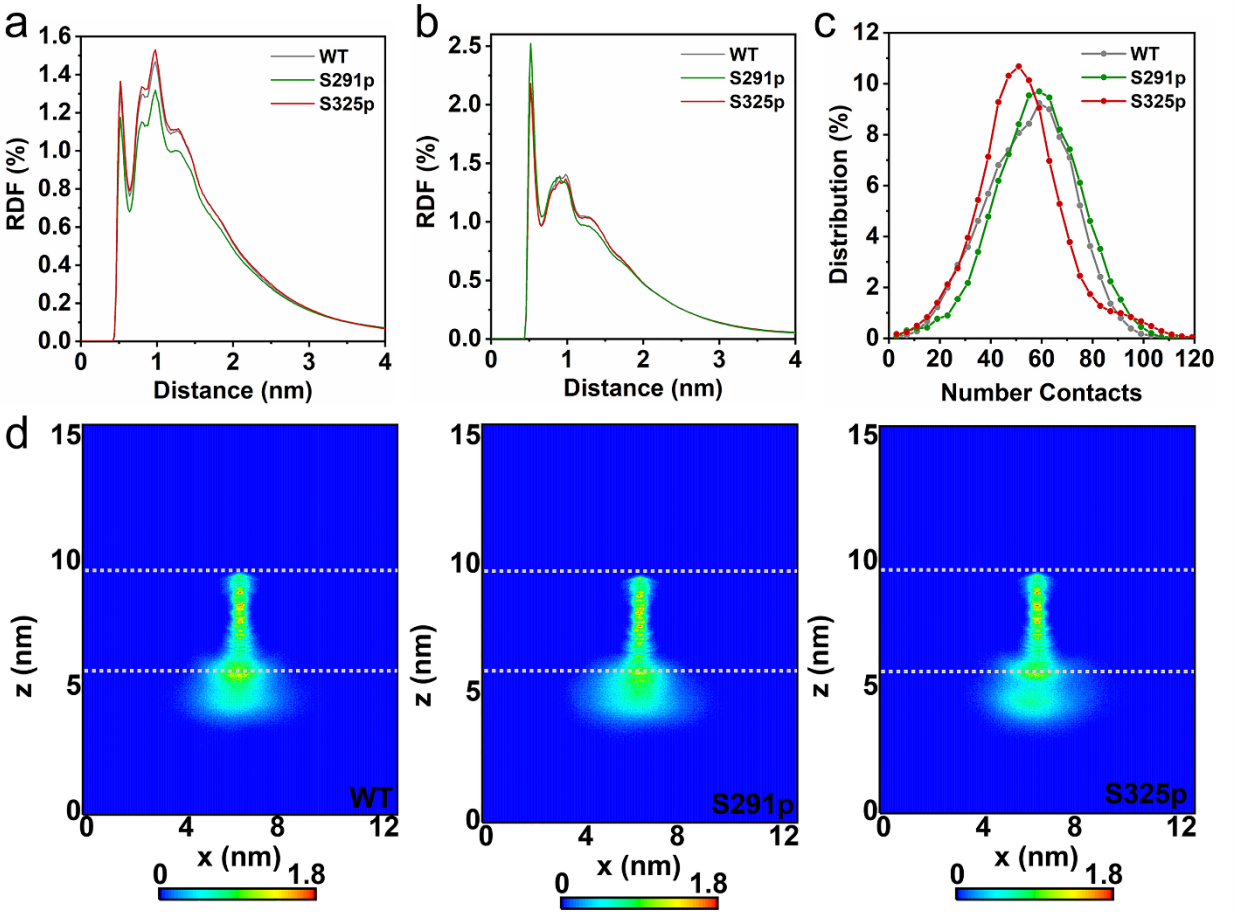

FIGURE S9. Interactions of CD44 with lipid phosphate in systems 95% POPC/5% PIP2 without FERM. (a) A comparison of radial distribution functions (RDF) of PIP2 lipids relative to CD44-TMD under different phosphorylation modifications. (b) A comparison of RDF of PIP2 lipids relative to CD44-CTD under different phosphorylation modifications. (c) Protein-lipid contact distribution of the CTD with the PIP2 under different phosphorylation. (d) The lateral density maps of the CD44-WT (left), CD44-S291p (middle) and CD44-S325p (right) relative to the lipid headgroups in systems without FERM. The gray dashed line shows the average position of the lipid phosphate head groups.

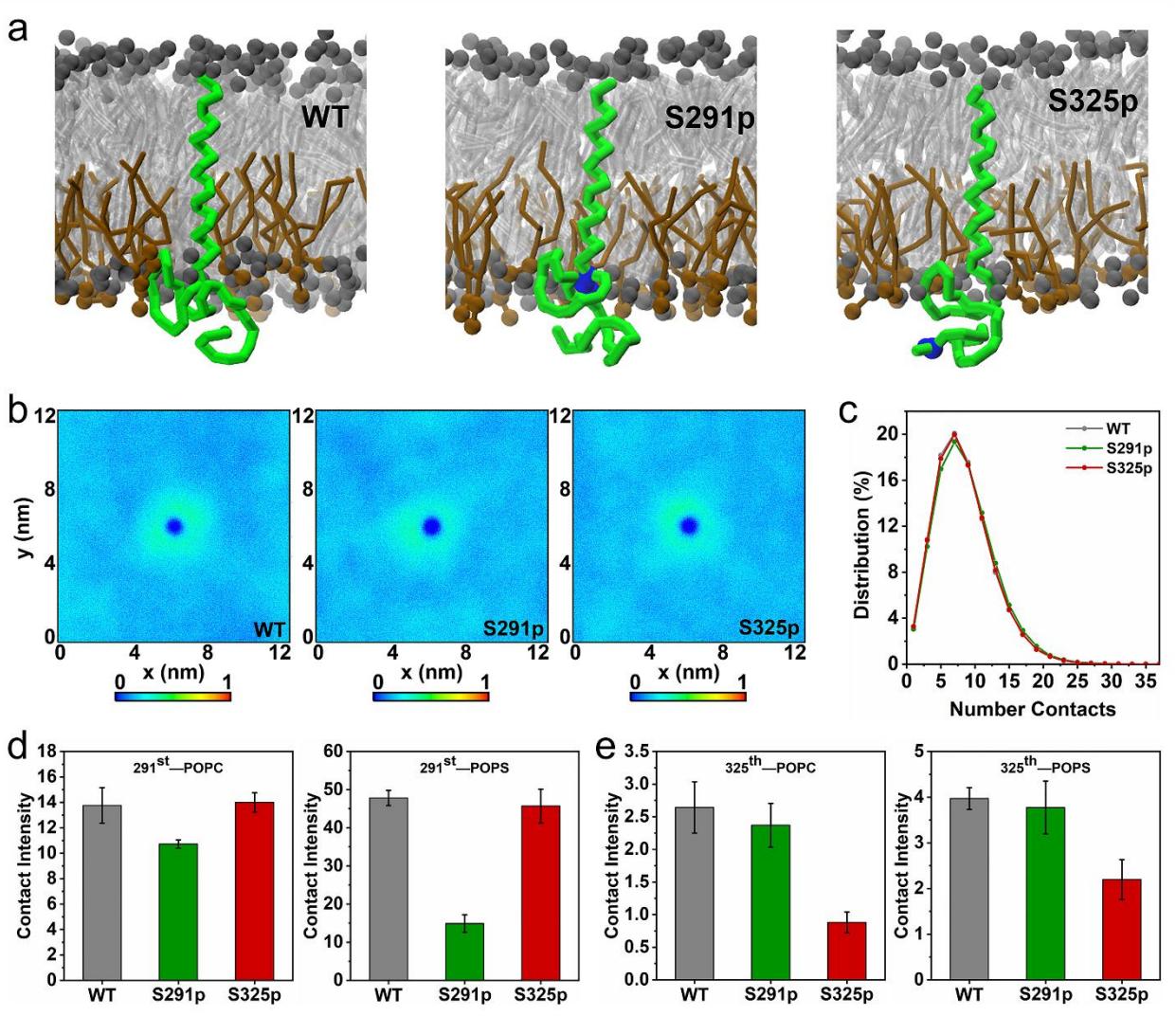

FIGURE S10. Conformational characterization of CD44 with different phosphorylation states in 80% POPC/20% POPS membrane environment. (a) Representative conformations of CD44-WT, CD44-S291p and CD44-S325P in the 80% POPC/20% POPS. (b) Density maps of the distribution of POPS relative to the TMD. Results were obtained from averaging the last 2.5 μs of all ten replicas. The CD44 is prefixed in the box center for analysis. (c) Protein-lipid contact distribution of the CTD with the lipid phosphates of POPC under different phosphorylation. Contact intensity of (d) the 291st residue and (e) the 325th residue with lipid phosphates of POPC (left) and POPS (right) in the three phosphorylation states.

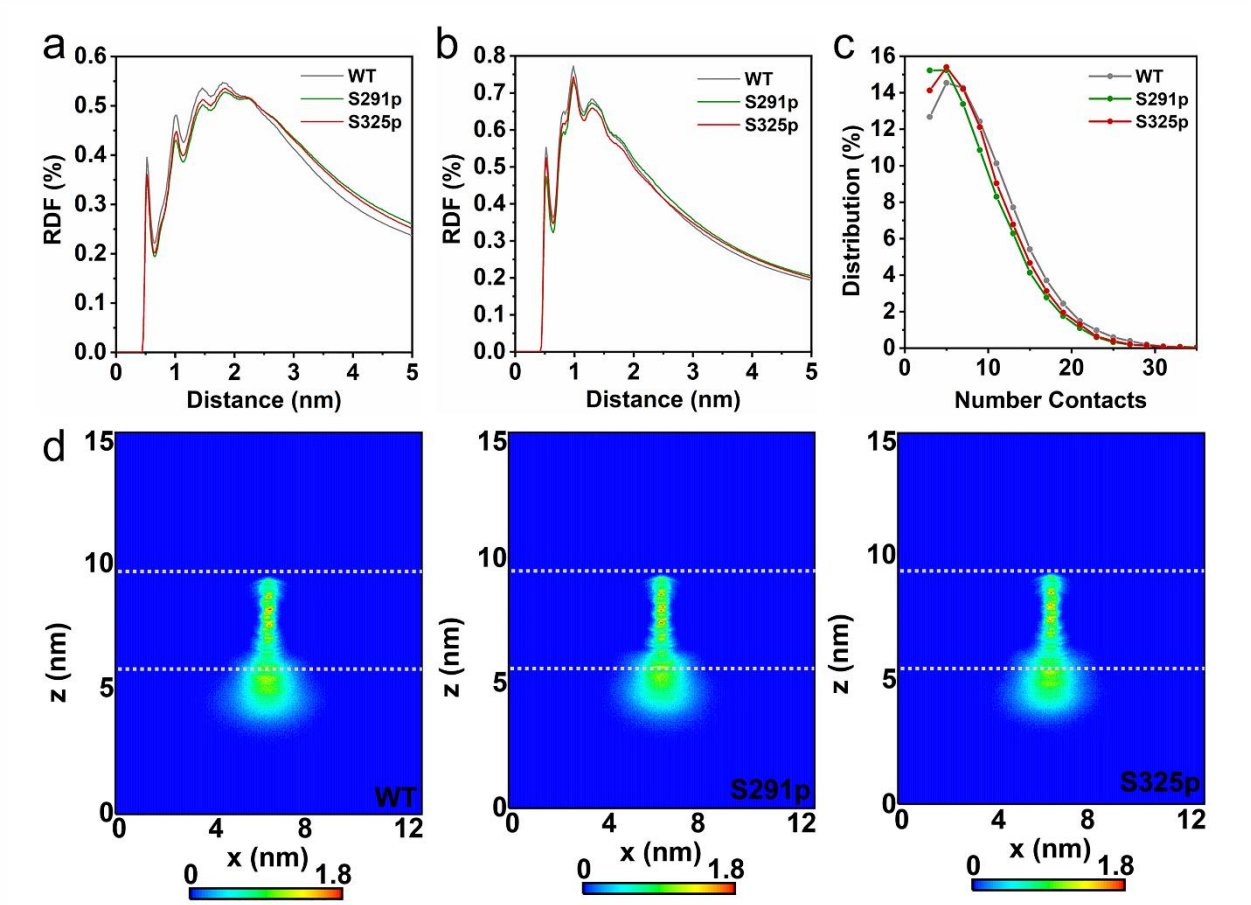

FIGURE S11. Interactions of CD44 with lipid phosphate in systems 80% POPC/20% POPS without FERM. (a) A comparison of RDF of POPS lipids relative to CD44-TMD under different phosphorylation modifications. (b) A comparison of RDF of POPS lipids relative to CD44-CTD under different phosphorylation modifications. (c) Protein-lipid contact distribution of the CTD with the POPS under different phosphorylation. (d) The lateral density maps of the CD44-WT (left), CD44-S291p (middle) and CD44-S325p (right) relative to the lipid phosphates of POPC in systems 80% POPC/20% POPS without FERM. The gray dashed line shows the average position of the lipid phosphate head groups.

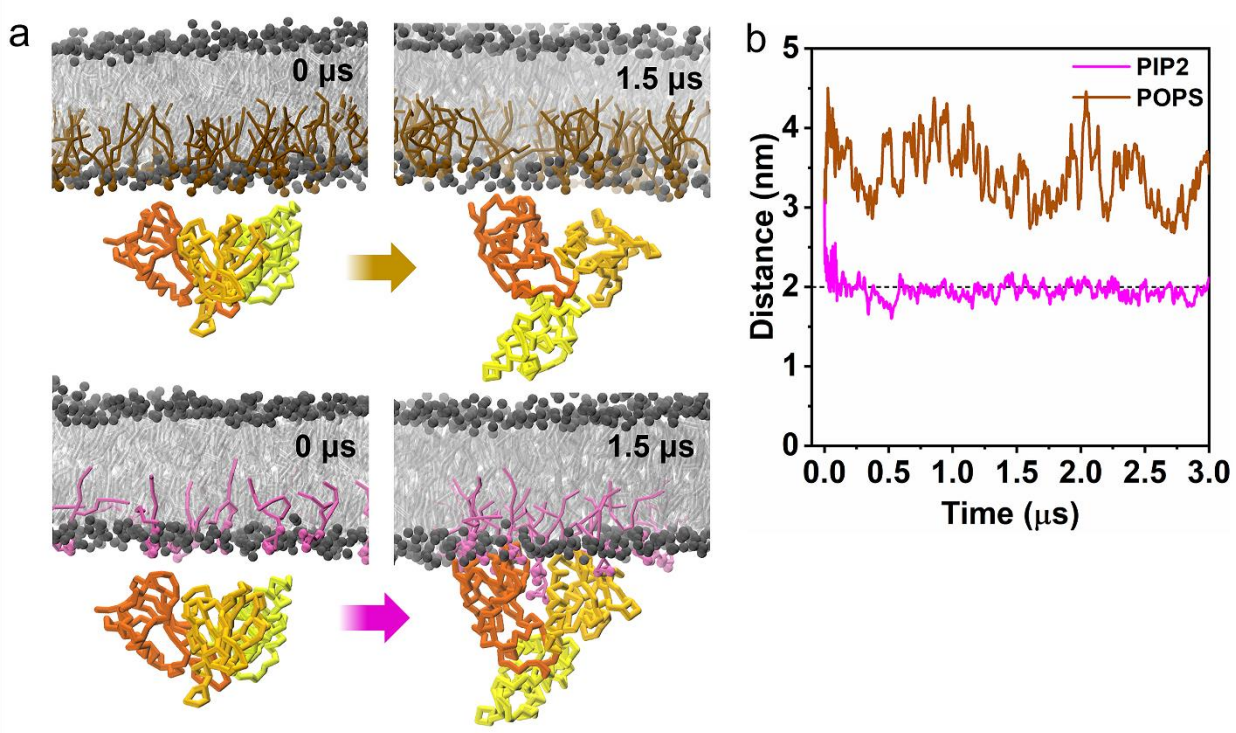

FIGURE S12. Location of FERM relative to different plasma membranes in a CD44-free system. (a) A snapshot of the position of the FERM relative to the membrane surface at the initial and after running for 1.5 μs, for membranes containing 95% POPC/5% PIP2 (left) and 80% POPC/20% POPS (right). (b) Distance evolution between the centers-of-mass of FERM and the lower lipid headgroups along the membrane normal with different membrane environment.

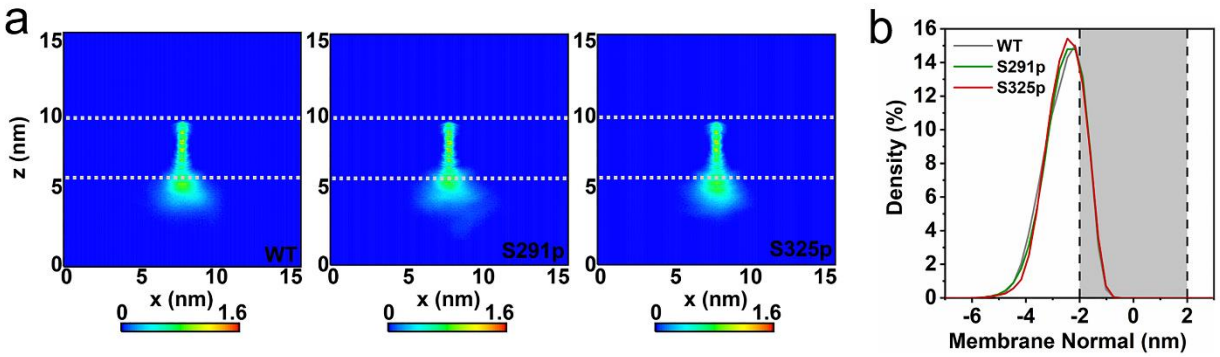

FIGURE S13. Density distribution of CD44 variants relative to the lipid phosphate moiety in systems 80% POPC/20% POPS with FERM. (a) The two-dimensional density maps of the CD44-WT (left), CD44-S291p (middle) and CD44-S325p (right) relative to the lipid phosphate moiety. The gray dashed line shows the average position of the lipid phosphate head groups. (b) The density distribution of the three phosphorylated CTDs along the membrane normal in the 80% POPC/20% POPS membrane system. (c) Density distribution of POPC lipid headgroups along the Z-axis of the box under different phosphorylation conditions.

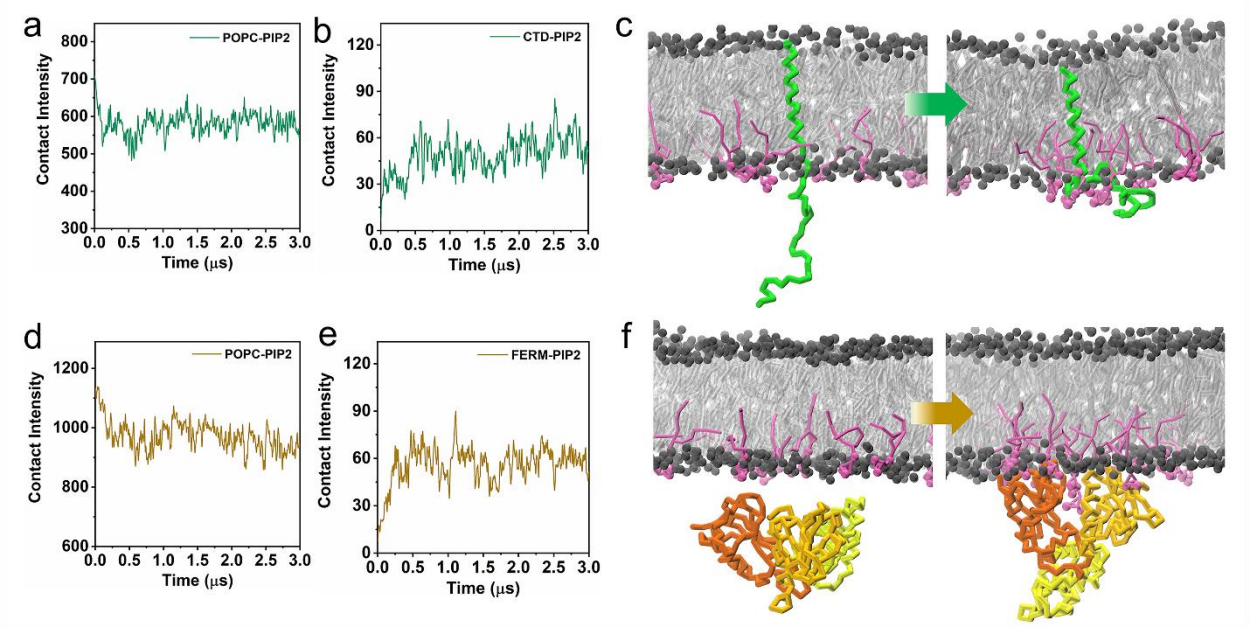

FIGURE S14. The aggregation of PIP2 lipid molecules aggregation affects protein binding to the inner leaflet of the plasma membrane. CD44 alone in the 95% POPC/5% PIP2 plasma membrane system, (a) evolution of the intensity of contact between POPC and PIP2; (b) Evolution of the intensity of contact between CD44-CTD and PIP2; (c) Schematic diagram of PIP2 aggregation and CTD and membrane adhesion. FERM alone in the 95% POPC/5% PIP2 plasma membrane system, (d) evolution of the intensity of contact between POPC and PIP2; (e) Evolution of the intensity of contact between FERM and PIP2; (f) Schematic diagram of PIP2 aggregation and FERM binding plasma membrane.